Nanostructures of polyelectrolyte gel-surfactant complexes in uniaxially stretched networks

Shigeo Sasaki,* Shogo Koga, Masaaki Sugiyama, and Masahiko Annaka

Department of Chemistry and Physics of Condensed Matter, Graduate School of Science, Kyushu University, 33 Hakozaki, Higashi ku, Fukuoka 812-8581, Japan

(Received 21 January 2003; published 18 August 2003)

Nanostructures of poly(acrylate) gel and dodecylpyridinium complexes equlibrated with the NaCl aqueous solution (from 5 to 100mM) and their time evolution after stretching uniaxially were investigated by means of time-resolved small-angle x-ray scattering. The scattering profile revealed the existence of the cubic nanostructure belonging to $Pm3n$ space group in the gel before and long after the stretch. Each of the three intensive peaks was found to be resolved into two, which suggested the existence of two cubic structures with the slightly different lattice spacings. On the other hand, the splits of scattering peaks were not observed for the linear poly(acrylate) and dodecylpyridinium complexes. This indicates that the existence of the cross-linked chain is concerned in the formation of the double structure in the complex system. A series of time-resolved experiments demonstrated that the peaks corresponding to the longer lattice constant disappeared once just after stretching and regenerated to grow up, whereas the peaks corresponding to the shorter lattice constant were continuously observed. The growing rates of the peaks increased with the NaCl concentration. It was also found that a two-dimensional scattering pattern changed from the Debye-Scherrer ring type into the Laue spot type with stretching at the lower NaCl concentrations. This indicates that the single-crystal-like domains align in the stretched network due to the strong electrostatic interaction between the dodecylpyridinium cation and poly(acrylate) anion.

I. INTRODUCTION

Ordered structures of soft materials microscopically and macroscopically found in the various biological systems such as lipid bilayers and DNA-protein complexes are mysterious but challenging objects to be investigated. The hydrophobic and ionic entities in the system have important roles in the formation of order. Ionic surfactant molecules can be highly condensed in the polyelectrolyte hydrogel and in the aqueous polyelectrolyte solution to make the polyelectrolyte surfactant complexes (PSC), which have recently attracted a great deal of attention, not only because of the fascinating physical mechanism to form the ordered structure [1,2] but also because of the potential application as nanoporous templates of inorganic solids [3].

The ordered nanostructures are also found in the surfactant solution at the concentration higher than 40 w/w%, even if polyelectrolyte chains are absent [4]. It might be considered that the roughly equal-sized micelles in the surfactant solution electrostatically repel with each other to array in an ordered manner like colloid crystals [5,6]. However, in the PSC, the electrostatic repulsive interaction between the micelles might be much shielded by the super-multivalent counterions of the polyelectrolyte chains. The charged chains are much condensed by the existence of oppositely charged micelles between them. What difference exists between the nanostructures in the PSC and the simple solution?

The deformation of the PSC in the polyelectrolyte gel (PSCg) produces the large and slow stress relaxations [7]. The large stress responding to the deformation reflects on the

solidlike nature of PSCg, and the slow relaxation of stress reflects on its liquidlike nature. The mechanical properites of the PSCg could orignate from the ordered structure in the PSCg. However, the kinetic behavior of the nanostructure in the deformed PSCg network is still unresolved and fascinating to reveal.

The PSC are also formed in the precipitates of linear polyelectrolytes bound by the surfactant ion (PSCp). Little difference between PSCp and PSCg is observed with respect to the boundaries between the formation and dissociation of PSC in the phase diagram for the salt (C_s) and the surfactant concentrations [8,9]. It has been revealed that there exists the critical salt concentration above which both the PSCg and PSCp cannot form even though the micelles exist in the solution [8,9]. This indicates an essential role of the electrostatic interaction to play in forming the ordered structures in the PSC. It has been revealed that the high charge density of polymer chains and the low cross-linker density are necessary conditions for forming the ordered nanostructures in the PSCg [10,11]. The high charge density of chains induces the highly condensed state of surfactant ions due to the electrostatic attraction. The low flexibility of chains due to the high cross-linker density and/or a star-like structure of crosslinked chain is not favorable for forming the ordered structure in the PSCg. What is induced in the ordered structures of PSC by changing the interaction between the surfactant ions and polyelectrolyte chains?

We have recently found that the Young's modulus of PSCg system at a NaCl concentration lower than 50mM is about ten times as high as that at $C_s = 100$mM [7]. This suggests that the shielding effect of salt on the electrostatic attraction between the chains and the surfactant ions seriously changes the structures of the PSC. However, much is not known about what occurs in the ordered structure with

---

*Author to whom correspondence should be addressed. Electronic address: s-sskscc@mbox.nc.kyushu-u.ac.jp

reducing the strength of electrostatic interactions by adding a simple salt to the PSC. In the present experiments, the deformation effect of the polyelectrolyte chains on the ordered nanostructures was examined by the time-resolved small-angle x-ray scattering (SAXS) patterns obtained for the PSCg at various salt concentrations. The C_s dependence of the structures of PSCg and PSCp was also examined to find out the difference between them.

II. EXPERIMENT

The poly(acrylate) gels were prepared by the radical co-polymerization [12] in the aqueous solution of $1M$ acrylic acid and $0.01M$ N,N'-methylenebis(acrylamide) at $60\,°C$. The gel synthesized in the space between two glass plates separated by a 1-mm-thick spacer of poly(tetrafluoroethylene) sheet was cut into about (20×10)-mm^2 rectangular plates and soaked in a $1M$ HCl aqueous solution. The gel was rinsed with water thoroughly, dried, and used. A small amount of $4N$ NaOH aqueous solution was put on the dry gel in order to fully ionize it. After homogeneously swelling the gel, the small amount of about $1M$ dodecylpyridinium chloride aqueous solution, which was the same mole amount of the carboxyl group in the gel, was put on the gel to soak into. Then the transparent gel became turbid. It took a few days for the turbid gel to be transparent. The gel was immersed into a large amount (about 20 ml) of $5mM$ dodecylpyridinium chloride aqueous solution of a given C_s. For achieving the equilibration, at which the turbid gels became transparent, the gel in the solution was kept at $50\,°C$ for more than a week and at room temperature for one day before the SAXS measurement. The gel size at this stage was roughly $20 \times 10 \times 1$ mm^3.

The PSCp was formed with mixing $0.3M$ sodium polyacrylate (Wako Pure Chemical Industries, Ltd.) and $0.3M$ dodecylpyridinium chloride solutions. The molecular weight of polyacrylate was more than $1\,000\,000$ according to the supplier. The obtained PSCp was similar to a highly viscous gum. The gumlike PSCp was immersed into a large amount (more than 100 times as large as the volume of PSCp) of dodecylpyridinium chloride (5 mM) and NaCl (a given concentration) aqueous solution. The gumlike character was held in the solution. For achieving the equilibration, the PSCp was kept in the solution at $80\,°C$ for more than a few days, during which the solution outside PSCp was exchanged with the fresh solution several times. The PSCp was kept at a room temperature for one day before the SAXS measurement. All chemicals used were of analytical grade. Double distilled water was used.

The time-resolved SAXS experiment was carried out with the SAXS spectrometer of BL45XU-A (RIKEN beamline I), installed at Spring-8 of Japan Synchrotron Radiation Research Institute, Hyogo, Japan. An incident x-ray beam from the synchrotron orbital radiation was monochromatized to 0.1 nm. The scattered x ray was detected by a two-dimensional (2D) position-sensitive detector (x-ray image intensifier plus charge coupled device CCD, Hamamatsu photonics ltd.) located at 2.3 m from the sample; the magnitude of the observed scattering vector q ranged from 0.07 to
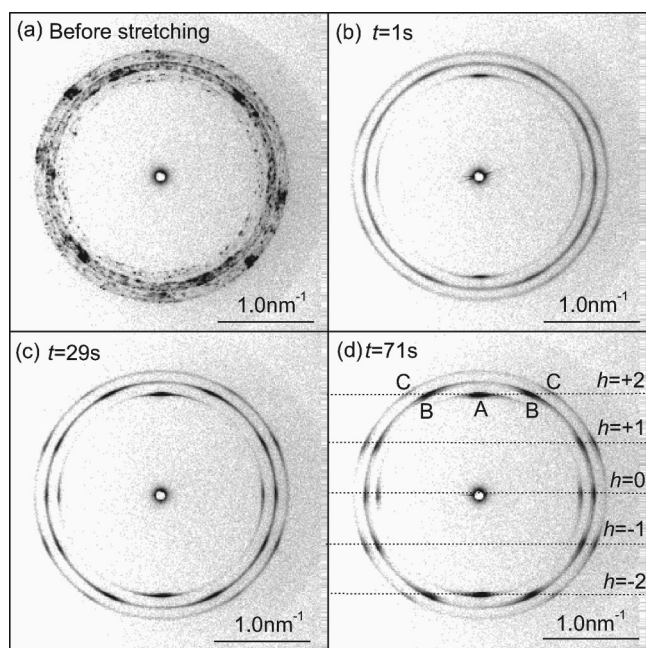

FIG. 1. Time-resolved two-dimensional SAXS images of PSC with $C_s = 5mM$ taken (a) before stretching; (b) at $t = 1$ sec, just after stretching; (c) at $t = 29$ sec; and (d) $t = 71$ sec. The stretching direction is vertical. The broken lines in panel (d) indicate the layer lines; diffraction spots of $A(200)$, $B(210)$, $C(211)$ belong to the same rings in the reciprocal space, respectively (see text).

2.5 nm^{-1}. The 2D-SAXS patterns with an exposure time of 500 msec were sequentially obtained for 140 sec with 7 sec intervals. The gel was stretched at 1 sec before the second exposure. The SAXS measurements were carried out at a room temperature. The elongation ratio of the stretched gel was about 2.

The SAXS measurements of PSCp were carried out at room temperature with the SAXS apparatus installed at BL10C of Photon Factory at the Institute of Materials Structure Science (IMSS), High Energy Accelerator Research Organization (KEK), Tsukuba, Japan. An x-ray beam from a synchrotron orbital radiation (0.1488 nm in wavelength) was used as a light source of the SAXS measurement; the magnitude of the observed scattering vector q ranged from 0.07 to 2.2 nm^{-1}. The spectra of the scattered x ray were obtained by using a one-dimensional position-sensitive detector.

III. RESULTS

Figure 1 shows the time-resolved two-dimensional SAXS images at a time before, just after, and long after stretching the gel at $C_s = 5mM$. Before the stretch [Fig. 1(a)], a lot of scattering spots were widely distributed on concentric circles. This indicates that the symmetry axes of domains, each of which has a single-crystal-like structure, are randomly oriented in the PSCg. In order to indentify the structure in the domain, an azimuthal average is taken for Fig. 1(a). As shown in Fig. 2, five peaks are observed in the averaged one-dimensional scattering profile. The relative po-
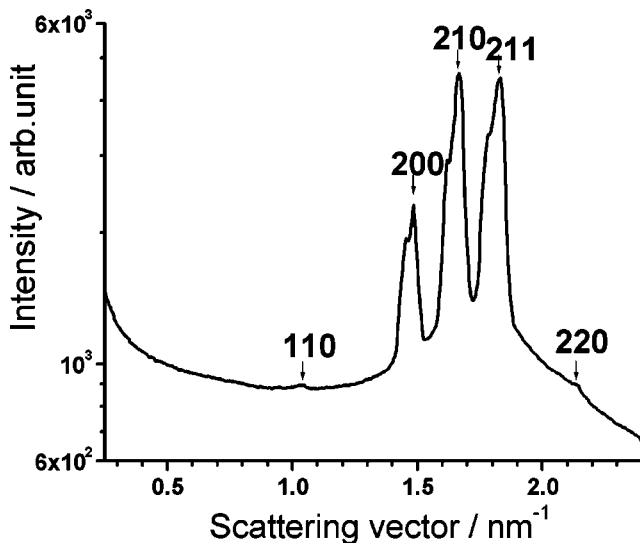
FIG. 2. Scattering profile of PSCg before stretching at $C_s = 5$mM. The peaks were indexed assuming a cubic structure with $a = 8.5$ nm.

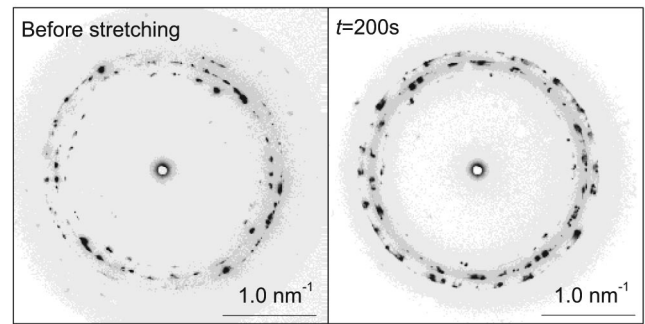

FIG. 3. Time-resolved 2D-SAXS images taken from PSCg with $C_s = 100$mM before stretching (left) and at $t = 200$ sec after stretching (right).

sitions of the peaks are in good agreement with a cubic structure belonging to the $Pm3n$ space group as indicated in Table I. The $Pm3n$ cubic structure has been reported in the other PSC systems [4,11]. The details of $Pm3n$ cubic structure cannot be determined from the present experiment and has been discussed elsewhere [14]. The cubic structure is supposed to be composed of discontinuous prolate micelles [15] and/or of bicontinuous surfactant aggregates [16].

It is remarkable that the stretch of the gel annihilates a lot of spots widely distributed over the ring belts and generates the regularly distributed spots on narrower rings as shown in Fig. 1. However, the relative peak positions observed in the one-dimensional scattering profiles (not shown) obtained by azimuthally averaging the 2D images of Figs. 1(b)–1(d) held same ratios as indicated in Table I, suggesting that the structure is still cubic belonging to $Pm3n$. The intensities of the appearing spots increase with time and, at $t = 71$ sec (t is a time elapsed after stretching), each of the spots becomes definite [Fig. 1(d)] and the regular spot pattern also becomes clear. The regular spot pattern suggests the alignments of the domains in the PSCg system. However, the spot pattern shown in Fig. 1(d) is not the scattering from a large single crystal but is the scattering from a number of crystals because 200 [spot A in Fig. 1(d)], 210 [spot B in Fig. 1(d)], and

TABLE I. Diffraction peaks indexed to the $Pm3n$ space group.

	Observed			$Pm3n$	
No.	q/nm^{-1}	Ratio	Order	Index	Ratio
1	1.05	1.00	1	110	$1.00(=\sqrt{2/2})$
2	1.48	1.41	2	200	$1.41(=\sqrt{4/2})$
3	1.67	1.59	3	210	$1.58(=\sqrt{5/2})$
4	1.83	1.74	4	211	$1.73(=\sqrt{6/2})$
5	2.13	2.03	5	220	$2.00(=\sqrt{8/2})$

211 [spot C in Fig. 1(d)] reflections never coexist on a same scattering plane in the case of diffraction from a single cubic crystal. For explaining the 2D scattering patterns [Figs. 1(c), 1(d)] after stretching, it could be assumed that one principal axis of each single crystallike domain, say p axis, is parallel to the stretching direction and that the other axes are randomly oriented on the plane perpendicular to it. Looking at the reciprocal space (h,k,l) under this assumption, the traces of the reciprocal lattice points of the $Pm3n$ cubic crystal rotating around the p axis form concentric circles on the same h plane. The crossing points of the concentric circles and the Ewald sphere can be observed as diffraction spots. For example, on the plane of $h = 2$ in the reciprocal space, the center point is 200 on the rotational axis, and the first circle consists of 210, 201, $2\bar{1}0$, and $20\bar{1}$, and the second one does 211, $21\bar{1}$, $2\bar{1}1$, and $2\bar{1}\bar{1}$: the center point, and the crossing points of the first and the second circles correspond to A, B, and C in Fig. 1(d), respectively. In like manner, we can assign all Miller indices of the diffraction spots in Fig. 1(d). This result strongly supports our assumption: the stretched PSC at $C_s = 5$mM is composed of the multidomains, one axis of which orients to the stretching direction. An uniaxial stretch of a gel network in PSCg induces an alignment of the domains to the stretching direction.

Figure 3 shows the stretching effect on the two-dimensional SAXS images of the gel at $C_s = 100$mM. It is obviously different from the images of the case $C_s = 5$mM shown in Fig. 1 that the randomness in the spot distributions over the three concentric circles holds after stretching. The assignment of the spots shown in Fig. 3 to Miller index is impossible. This is different from the case $C_s = 5$mM.

It is a common feature in the time-resolved SAXS images shown in Figs. 1(b)–1(d) and 3 that the belts over which the scattering spots are distributed widen with t elapsing after the stretch. Two peaks are distinguishably observed in each spot of the 2D scattering images, indicating the existence of two ordered nanostructures with different lattice constants.

The 2D scattering images of the nonstretched PSCg at $C_s = 5, 50,$ and 100mM are averaged over the azimuthal directions to show as the scattering spectra in Fig. 4, which also shows the scattering spectra of PSCp for comparison. More than one peak, mainly two peaks, are seen at each spot in the spectra of PSCg, while only one peak is seen at each
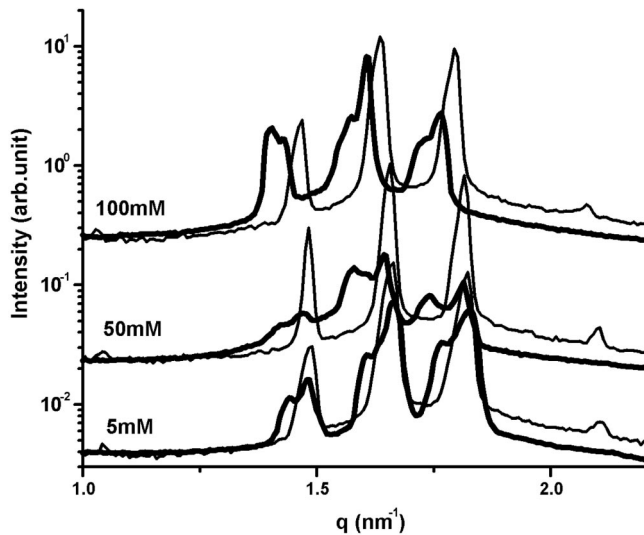
FIG. 4. Scattering spectra of PSCg (thick lines) and PSCp (thin lines) at several salt concentrations before stretching.

spot in the scattering spectra of PSCp at $C_s = 5$, 50 and 100mM as shown in Fig. 4. The existence and absence of a cross-link in the PSC chain might cause the difference between the spectra mentioned above. It should be mentioned here that the peak intensities of 110 and 220 of PSCg can be observed as very weak spots in the 2D image, although their averaged intensities are relatively too small to appear as peaks in Fig. 4.

Figure 5 shows the C_s dependence of lattice constants, a estimated from the three intensive peak positions, q (200,
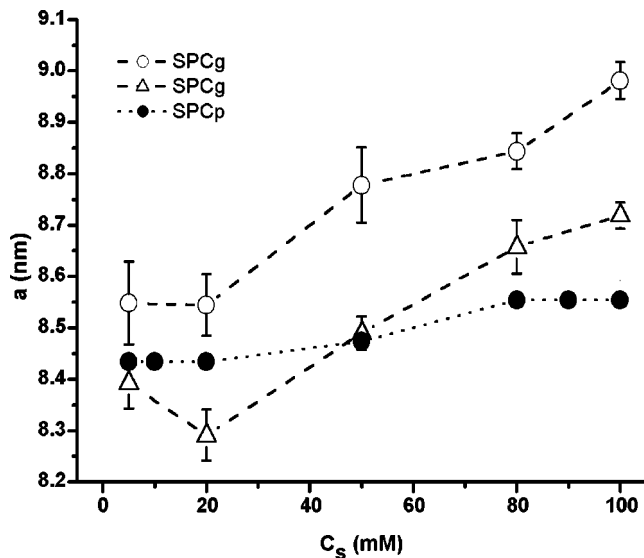

FIG. 5. Salt concentration dependences of lattice constants of PSCg (open symbols) and PSCp (closed symbols). The large and small lattice constants of PSCg are represented by the circles and triangles, respectively. The lattice constants of PSCg evaluated for more than ten spots are within the error bars. The lattice constants of PSCp evaluated from the three peak positions shown in Fig. 4 are within the symbols. Broken dotted lines are drawn to guide the eyes.
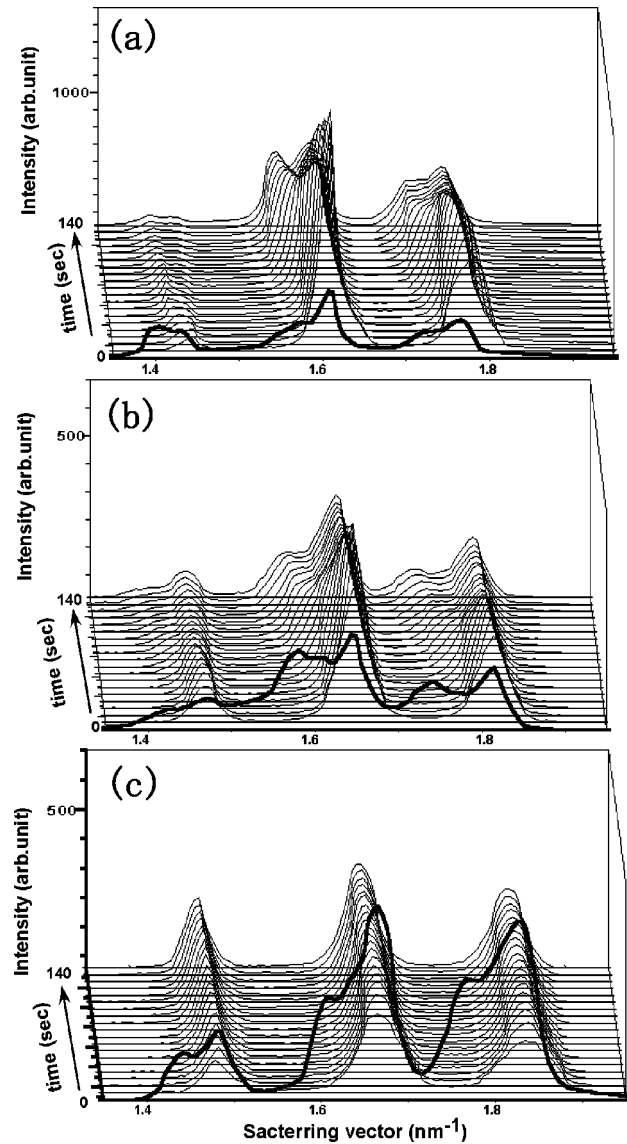

FIG. 6. Time-resolved spectra averaged over the azimuthal directions of the 2D scattering images: (a) $C_s = 100$mM, (b) $C_s = 50$mM, and (c) $C_s = 5$mM. Thick lines show the scattering profile just before stretching.

210, and 211 reflections). The $Pm3n$ cubic assumption for two lattices in PSCg is rationalized by the consistent a values for the different peak positions. The a values of PSCg and PSCp significantly increase with C_s in the C_s region higher than 20mM as shown in Fig. 5. It is worthwhile to point out that the SAXS spectra with lower q resolution than the present experiment might hide the multiple peaks of PSCg and the C_s dependent a of PSCp.

Figure 6 shows the time-resolved spectra, which are averaged over the azimuthal directions of the 2D scattering images of the PSCg at $C_s = 5$, 50, and 100mM. The peaks corresponding to the cubic structure with a larger a disappear in stretching the gel and reappear with time elapsing after the stretch. The reappearance times are about 20 sec at $C_s = 50$ and 100mM, and are longer than 100 sec at $C_s = 5$mM. The peaks for the cubic structure with a small a appear within
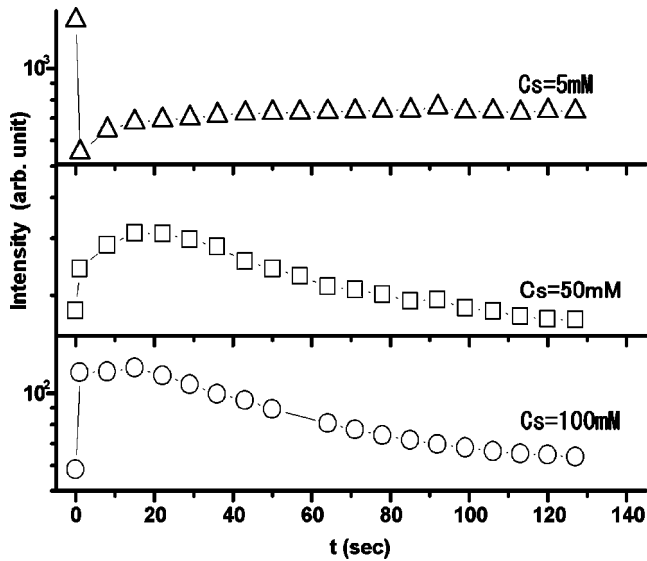
FIG. 7. Time profiles of the peak intensities of the 210 reflection from the cubic structure with the small lattice constant.

1 sec after stretching or they continuously appear during stretching.

Figure 7 shows time profiles of the intensities of 210 reflection corresponding to the cubic with the small lattice spacing. In stretching the gel, the peak intensity increases at $C_s = 50$ and 100mM, but decreases at $C_s = 5$mM. The peak intensity at $C_s = 50$mM increases until $t = 22$ sec, as in the case of $C_s = 5$mM, and then decreases, as in the case of $C_s = 100$mM. The decrease in the intensity is consistent with the decrease in the scattering volume with stretching. However, the decrement of peak intensity at $C_s = 5$mM, 0.6, cannot be explained by the reduction of the scattering volume alone, since the elongation ratio of 2 in the present experiment leads to the decrement of $1 - 1/\sqrt{2}$ (~ 0.3). The increases of the peak intensity at $C_s = 50$ and 100mM are contradictory to the reduction of scattering volume. The causality for the discrepancies will be discussed in the following section.

IV. DISCUSSION

In this section, the experimental results are interpreted by taking the NaCl concentration (C_s) dependence of the Young's modulus of PSCg system [7] into consideration. The fact that the Young's modulus at C_s lower than 50mM is about ten times as high as that at $C_s = 100$mM indicates that the network in the PSCg at the low C_s is more rigid than that at the high C_s. The rigid structures of PSCg are due to the network structure of the polyelectrolyte chains tightly wound around the surfactant aggregates, since the electrostatic attraction between the opposite charges is strong at the low C_s. The loose pairing of the chains and aggregates at the high C_s makes the network soft.

In uniaxially stretching the gel network, the mesh of ionized chains expands in the stretching direction and shrinks in the direction perpendicular to it. The 2D SAXS images of Fig. 1 show that the surfactant aggregates array along the stretching direction at $C_s = 5$mM. This suggests that the polyelectrolyte network chains and the long axis of spheroidal surfactant aggregates tend to align to the stretching direction. It is plausible that the polyelectrolyte chains tightly wound around the surfactant aggregates align along the stretching direction. It should be notified that the spots from the stretched PSCg at $C_s = 100$mM shown in Fig. 3 are randomly distributed on the Debye-Scherrer rings. The aggregates loosely wound by chains at the high C_s are not aligned along the stretching direction.

It has been revealed that the concentrations of dodecylpyridinium (DP) ion and chains in the PSCg decrease with C_s [7]. The increase of C_s weakens the electrostatic attraction between the surfactants and the charged chains [17], which tends to expand the PSCg because of their entropy force. The lattice spacing increases with the water content in PSC [19], which increases with the decrease of concentrations of the surfactant molecule and the chain. As a matter of fact, the lattice spacing of PSCg increases with C_s as shown in Fig. 5. The lattice spacing of PSCp also gradually increases with C_s as shown in Fig. 5. This suggests that the concentrations of the surfactant ion and the polyelectrolyte chain in PSCp tend to decrease with C_s.

It is interesting that the lattice spacing of PSCg is significantly larger than that of PSCp at C_s higher than 50mM, as shown in Fig. 5. This suggests that the chain concentration C_p in the PSCg is lower than that in the PSCp. C_p can be approximately described as follows [13]:

$$C_p \sim n^{1-3\nu}, \tag{1}$$

where n and ν, respectively, are an effective segment number of a statistically independent chain (a blob) and the Flory exponent of the chain. C_p generally decreases with n, since the ν value is always greater than 1/3. C_p decreases with ν for a constant n. The difference between C_p in the PSCg and the PSCp suggests that the n value and/or ν value of PSCg are larger than that or those of PSCp. The difference between PSCg and PSCp should be explained by the existence or absence of cross-linked chains in the PSC. Although the excluded volume effect of segments near the cross link might increase the ν value, a true mechanism for the cross link to increase the n value and/or the ν value cannot be revealed from the present experiment. At least we can say that the cross-linked chains in the PSCg tend to expand when the shielding effect of salt weakens the electrostatic condensing force for the ionic chains and the surfactants. In the salt-free condition, the difference between the lattice spacings of structures in PSCg and PSCp is so small as has been observed in the hexagonal structures of PSCg (4.6–4.9 nm) and PSCp (4.6 nm) of cetyltrimethylammonium (CTA) and polyacrylate (PA) system [22,18].

The existence of two types of chains, the cross-linked and dangling chains, in the gel network should be taken into consideration in explaining the two cubic structures with different lattice constants as shown in Figs. 4 and 5. The dan-

gling and linear chains have free chain ends and their conformations are similar to each other. From this similarity, C_p of the dangling chain is inferred to be close to that of the linear chain and higher than that of the cross-linked chain. It is plausible that the existence of the dangling chain causes the smaller lattice spacing of PSCg being close to that of PSCp as shown in Fig. 5. The inhomogeneous distribution of cross-linked and dangling chains in poly(acrylate) gel over the wavelength of light is suggested by the nonergodic properties observed in the light scattering experiments [20].

The uniaxial stretch of the gel network makes the conformations of the cross-linked and dangling chains more expanded along the stretching direction. These conformational changes might disturb the ordered structures to change their domain fraction. The ordered structure forming around the cross-linked chain is more flexible than that around the dangling chain, since the former is supposed to be less condensed. The flexible parts are generally more deformative than the rigid parts. Therefore, the ordered arrays in the cross-linked chain rich domain tend to change or be in disorder with stretching. C_p in the cross-linked chain rich domain slightly increases, which homogenizes the rigidity of the PSCg system. The stretch of the gel tends to increase the concentrations of surfactant molecule and chain in the cross-linked chain rich domain. The temporal increase of C_p in the cross-linked-chain rich domain leads to the apparent increase of domain fraction of ordered array with the small lattice spacing, if the ordered structures are flexible as a whole. A less constrained structure is more flexible, which is realized by weakening the electrostatic attraction between the chains and surfactant molecules. This is observed as the initial increase of the peak intensity corresponding to the structure with the small lattice spacing at $C_s = 50$ and 100mM, as shown in Fig. 7. The stretch tends to make the structures formed by the strong electrostatic attraction between the chains and surfactant molecules be in disorder, since the stretched conformations of the chains initially might be somehow different from the chain conformations in the ordered structures at the rest state. Therefore, the peak intensity corresponding to the structure with the small lattice spacing at $C_s = 5$mM decreases initially as shown in Fig. 7.

As the time elapses after stretching, the conformation of the dangling chain changes from the extended to the globulelike form, and the cross-linked chains expand again to decrease the concentrations of surfactant molecules and chains in their domains. As a result of decrease of the concentrations in the cross-linked chain rich domain, the lattice spacing there increases. The domain fraction occupied by the structure with the small lattice spacing gradually decreases and the corresponding peak intensity also decreases. The spot diffracted from the structure with the large lattice spacing gradually appears. The former is seen in the bottom graph ($C_s = 100$mM) of Fig. 7 and the latter in Fig. 6(a) ($C_s = 100$mM). In the case of the low C_s, the conformational change of the dangling chain and the induction of the ordered structure are time consuming processes because of the high rigidity of the structure [7]. This reflects on the gradual increase of the intensity diffracted from the structure with the small lattice spacing as shown in the uppermost graph of Fig. 7 ($C_s = 5$mM).

The growing rates of the peak intensities corresponding to the cubic structure with large lattice spacing increase with the increase in C_s as shown in Fig. 6. This indicates that the cubic structure at high C_s forms faster than that at low C_s, since the peak intensity is proportional to the domain fraction of the corresponding ordered structure. The cross-linked and dangling chains in the PSCg deform to lengthen in the stretching direction just after stretching the gel network. Only the dangling chain can shrink to minimize the conformational energy because one of its ends is free to move. The shrinking process of dangling chains can be observed as the relaxation of elastic force of the gel [7,21]. The final ordered structures appear after settling the movement of dangling chains. The reappearing peaks corresponding to the structure with the large lattice spacing at $C_s = 50$ and 100mM, as shown in Fig. 6, are due to the ordered structures reformed in the cross-linked chain rich domain as explained above. The time profiles of the peak intensities for the larger lattice spacing, as shown in Fig. 6, demonstrate that the settling times of cross-linked chains at $C_s = 50$ and 100mM are about $t = 100$ sec and that the chains at $C_s = 5$mM are not settled at $t = 120$ sec after the stretch. The orders of these times are comparable to the relaxation times of the excess moduli [7].

V. SUMMARY

The following facts are revealed by the present SAXS measurements of PSC at various C_s: (a) two cubic structures with different lattice spacings are found in the PSCg, while one cubic structure is found in the PSCp; (b) in stretching the gel, one of the principal axes of the cubic structures in PSCg at a low salt concentration such as $C_s = 5$mM align to the stretching direction; (c) the lattice constants of the cubic structures in both of the PSCg and PSCp increase with C_s; (d) the lattice constants of the structures in PSCg are significantly larger than those in PSCp at C_s higher than 50mM; (e) the cubic structures with large lattice spacings broken with the stretching are reconstructed at about 20 sec at $C_s = 50$ and 100mM and a time longer than 100 sec at $C_s = 5$mM; (f) the cubic structures with small lattice spacings are consistently held or reconstructed within 1 sec after stretching; (g) in stretching the gel, the domain fractions of cubic structures with small lattice spacings increase at $C_s = 50$ and 100mM and decrease at $C_s = 5$mM; (h) with time elapsing after the stretch, the domain fractions of cubic structures with small lattice spacings decrease at $C_s = 50$ and 100mM and increase at $C_s = 5$mM.

The C_s dependent behavior of PSC can be explained by the shielding effect on the electrostatic attraction between the ionized chains and micelles. The structures with large lattice spacings in PSCg are explained by the existence of cross-linked chains in the gel, which is suppose to expand the collapsed network.

[1] Yu.V. Khandurina, A.T. Dembo, V.B. Rogacheva, A.B. Zezin, and V.A. Kabanov, Polym. Sci., Ser. A Ser. B **36**, 189 (1994).

[2] E.L. Sokolov, F. Yeh, A. Khokhlov, and B. Chu, Langmuir **12**, 6229 (1996).

[3] P.V. Braun, P. Osenar, V. Tohver, S.B. Kennedy, and S.I. Stupp, J. Am. Chem. Soc. **121**, 7302 (1999)

[4] R.R. Balmbra, J.S. Clunie, and J.F. Goodman, Nature (London) **222**, 1159 (1969).

[5] S. Hachisu and S. Yoshimura, Nature (London) **188**, 283 (1980).

[6] S. Sasaki and N. Imai, J. Phys. Soc. Jpn. **52**, 2571 (1983).

[7] S. Sasaki and S. Koga, J. Phys. Chem. B **106**, 11893 (2002).

[8] S. Sasaki, S. Koga, R. Imabayashi, and H. Maeda, J. Phys. Chem. B **105**, 5852 (2001).

[9] A.R. Khokholov, E.Yu. Kramanenko, E.E. Makhaecva, and S.G. Starodubtzev, Macromolecules **25**, 4779 (1992).

[10] S. Zhou, C. Burger, F. Yeh, and B. Chu, Macromolecules **31**, 8157 (1998).

[11] S. Zhou, F. Yeh, C. Burger, and B. Chu, J. Phys. Chem. B **103**, 2107 (1999).

[12] S. Sasaki, D. Fujimoto, and H. Maeda, Polym. Gels Networks **3**, 145 (1995).

[13] P. G. Degennes, *Scaling Concepts in Polymer Physics* (Cornell University Press, Ithaca, 1979), Chap. 5.

[14] K. Fontell, Colloid Polym. Sci. **268**, 264 (1990).

[15] P. Hansson, Langmuir **14**, 4059 (1998).

[16] S. Zhou, F. Yeh, C. Burger, B. Chu, J. Polym. Sci., Part B: Polym. Phys. **37**, 2165 (1999).

[17] K. Wagner, D. Harries, S. May, V. Kahl, J.O. Rädler, and A. Ben-Shaul, Langmuir **16**, 303 (2000).

[18] P. Hansson, S. Schneider, and B. Lindman, J. Phys. Chem. B **106**, 9777 (2002).

[19] P. Ilekti, T. Martin, B. Cabane, and L. Piculell, J. Phys. Chem. B **103**, 9831 (1999).

[20] A. Moussaid, A.J. Candau, and J.G.H. Joosten, Macromolecules **27**, 2102 (1994).

[21] S. Sasaki and S. Koga, Macromolecules **35**, 857 (2002).

[22] A. Svensson, L. Piculell, B. Cabane, and P. Ilekti, J. Phys. Chem. B **106**, 1013 (2002).